Research Article Vol. 4, No. 8 / August 2017 / Optica 940

1.3 μm submilliamp threshold quantum dot micro-lasers on Si

Yating Wan,[1,2] Justin Norman,[3] Qiang Li,[2] M. J. Kennedy,[1] Di Liang,[4] Chong Zhang,[4] Duanni Huang,[1] Zeyu Zhang,[1] Alan Y. Liu,[3] Alfredo Torres,[1] Daehwan Jung,[3] Arthur C. Gossard,[1,3] Evelyn L. Hu,[5] Kei May Lau,[2,6] and John E. Bowers[1,3,7]

[1]Department of Electrical and Computer Engineering, University of California Santa Barbara, Santa Barbara, California 93106, USA
[2]Department of Electronic and Computer Engineering, Hong Kong University of Science & Technology, Clear Water Bay, Hong Kong
[3]Materials Department, University of California Santa Barbara, Santa Barbara, California 93106, USA
[4]Hewlett Packard Labs, Hewlett Packard Enterprise, 1501 Page Mill Road, Palo Alto, California 94304, USA
[5]School of Engineering and Applied Sciences, Harvard University, Cambridge, Massachusetts 02138, USA
[6]e-mail: eekmlau@ust.hk
[7]e-mail: bowers@ece.ucsb.edu

Received 20 March 2017; revised 24 June 2017; accepted 7 July 2017 (Doc. ID 290829); published 4 August 2017

As a promising integration platform, silicon photonics need on-chip laser sources that dramatically improve capability, while trimming size and power dissipation in a cost-effective way for volume manufacturability. Currently, direct heteroepitaxial growth of III–V laser structures on Si using quantum dots as the active region is a vibrant field of research, with the potential to demonstrate low-cost, high-yield, long-lifetime, and high-temperature devices. Ongoing work is being conducted to reduce the power consumption, maximize the operating temperature, and switch from miscut Si substrates toward the so-called exact (001) Si substrates that are standard in microelectronics fabrication. Here, we demonstrate record-small electrically pumped micro-lasers epitaxially grown on industry standard (001) silicon substrates. Continuous-wave lasing up to 100°C was demonstrated at 1.3 μm communication wavelength. A submilliamp threshold of 0.6 mA was achieved for a micro-laser with a radius of 5 μm. The thresholds and footprints are orders of magnitude smaller than those previously reported lasers epitaxially grown on Si.

OCIS codes: (230.5590) Quantum-well, -wire and -dot devices; (140.5960) Semiconductor lasers; (140.3948) Microcavity devices; (160.3130) Integrated optics materials.

https://doi.org/10.1364/OPTICA.4.000940

1. INTRODUCTION

In analogy to the historical scaling of complementary metal-oxide-semiconductor (CMOS) technology governed by Moore's law, there is an enduring and increasing need for miniaturization and large-scale integration of photonic components on the silicon platform for datacom and emerging applications [1–6]. By confining light to small volumes with resonant recirculation, micro-lasers with low-loss, high-quality whispering gallery modes hold great promise for ultra-low-threshold lasing that is not limited by challenges in gratings or Fabry–Perot (FP) facets for optical feedback [7].

Based on a special GaAs-on-Si template design, we recently developed continuous-wave (CW) *optically pumped* micro-lasers operating at room temperature that were epitaxially grown on silicon with no germanium buffer layer or substrate miscut [8]. A quantum dot (QD)-based active medium can effectively alleviate the negative influence of dislocations and surface recombination arising from lattice-mismatched growth and device fabrication. Therefore, the micro-lasers exhibited ultra-low thresholds and good temperature characteristics in the 1.3 μm telecommunication band, comparable to identical devices simultaneously fabricated on a *native* GaAs substrate and showing great potential to serve as light sources for silicon photonic integrations [9].

Recently, electrical pumped FP lasers with QDs grown on (001) silicon have been reported under CW operation. Low thresholds of 36 mA and high heatsink temperature up to 80°C were achieved on a 6×1200 μm^2 ridge with the polished facets and high reflectivity coating [10]. However, electrical injection of micro-lasers is more challenging: the electrode metallization is limited by the micro size cavity, which may increase the device resistance and thermal impedance; the whispering gallery mode (WGM) is sensitive to any process imperfection that increases the optical loss. [11–13]. In this Letter, we demonstrate record-small electrically pumped QD lasers epitaxially grown on (001) silicon. CW lasing around 1.3 μm has been achieved with maximum operating temperatures up to 100°C. Scaling the micro-sized WGM cavity to a radius of 5 μm results in ultra-low thresholds down to 0.6 mA. Both the thresholds and footprint are much smaller than those previously reported lasers epitaxially grown on silicon [14,15].

2. GROWTH AND FABRICATION

The GaAs-on-Si template [Fig. 1(a)] was grown by metal-organic chemical vapor deposition with the method detailed in Ref. [16]. *V*-grooves along [100] direction were defined on (001) silicon substrates with the wet etch method using patterned SiO_2 as masks. An array of GaAs in-plane nanowires was first grown inside silicon *V*-grooves by selective-area heteroepitaxy. The 4.1% lattice mismatch between GaAs and silicon was mostly accommodated by the formation of a few nanometer-thick stacking faults in the *V*-grooved structure, as revealed by the cross-sectional transmission electron microscopy (TEM) images in Figs. 1(b) and 1(c). After removing the SiO_2, further GaAs growth, inlcuding 15 periods of $Al_{0.3}Ga_{0.7}As$/GaAs (5/5 nm) superlattice for annihilating the threading dislocations, was carried out. Eventually those GaAs nanowires were coalesced into a 1.5-μm-thick continuous and smooth surface with a root mean square roughness of 0.8 nm, as shown in a 10 μm × 10 μm AFM scan [Fig. 1(d)]. Analysis from the XRD omega-rocking curve showed a small full width at half-maximum (FWHM) value of 162 arcsec [Fig. 1(e)]. The GaAs/$Al_xGa_{1-x}As$ graded-index separate-confinement laser heterostructure was grown in a molecular beam epitaxy system. Seven InAs/InGaAs quantum dot-in-a-well layers were incorporated in the laser active region, with QD density around 6×10^{10} cm^{-2} [17]. A schematic of the complete epitaxial laser structure is shown in Fig. 1(f).

Figure 2(a) schematically highlights the critical processing steps in the device fabrication. The ring structures with radii ranging from 5 to 50 μm and ring widths 2 to 7 μm wide were patterned using an oxide hard mask deposited by plasma-enhanced chemical vapor deposition. The radius is defined as the center to the outer perimeter of the ring, and the ring width is defined as the width of the patterned ring mesa. Inductively coupled plasma etching was used to transfer the photoresist pattern to the SiO_2 hard mask, followed by a III-V deep etch all the way to the *n*-contact layer. The 4-μm-tall dry-etched mesa allows strong lateral optical confinement and therefore preserves the excellent cavity modes to enable the low-threshold lasing.

After metallization with Pd/Ti/Pd/Au and Pd/Ge/Au layer stacks to form the *p*- and *n*-contacts by *E*-beam evaporation, the sidewall was passivated with 12 nm atomic-layer deposited (ALD) Al_2O_3 to further reduce the sidewall surface recombination and diffusion. Then, a 1-μm-thick SiO_2 layer was sputtered to fully isolate the optical modes from the deposited metal pads. After via opening, contact probe pads were formed with *n*-contact pads displaced laterally around the ring mesa and *p*-contact on top of the ring mesa for efficient current injection and spreading. A fabricated device is presented through the top view [Fig. 2(b)] and cross-sectional view [Fig. 2(c)] scanning electron microscope (SEM) images. A 90° tilted zoomed-in SEM image in Fig. 2(d) clearly shows a smooth and steep mesa sidewall.

3. RESULTS AND DISCUSSION

Typical CW light current voltage (LIV) characteristics of a micro-ring laser with a radius of 50 μm and a mesa width of 4 μm are shown in Figs. 3(a) and 3(b). To measure the optical power, radiation out-coupling from the micro-laser cavity was collected by an integrating sphere at the side. The optical power magnitude presented here is thus an underestimated value, considering the angular directivity pattern of radiation. A low lasing threshold around 15 mA was measured, corresponding to a threshold current density (J_{th}) of 1.2 kA/cm^2. WGM resonators rely on the confinement of light by total internal reflection at curved boundaries, and the high-quality modes propagate mainly close to the cavity boundary. The cavity WGM is thus sensitive to any process imperfection contributing to the optical loss [11–13]. The situation is even more complicated considering the high aspect ratio of the sidewall/active region volume (~0.0768 $μm^{-1}$) in our structure. With yet to be fully optimized etching conditions, even surface passivation and the three-dimensional confinement of carriers in the QD active region resulted in higher non-radiative recombination and light scattering at the micro-ring sidewall compared to the large FP lasers [10] using the same material system. The J_{th} here is thus higher compared with the FP lasers, where the minimum value is 498 A/cm^2 [10].

Emission spectra of the micro-laser, measured at progressively higher pump currents from 15 to 80 mA, are presented in Fig. 3(c). Narrow lines as a result of WGM emission arise near the intensity maximum (~1.3 μm) of the ground-state optical

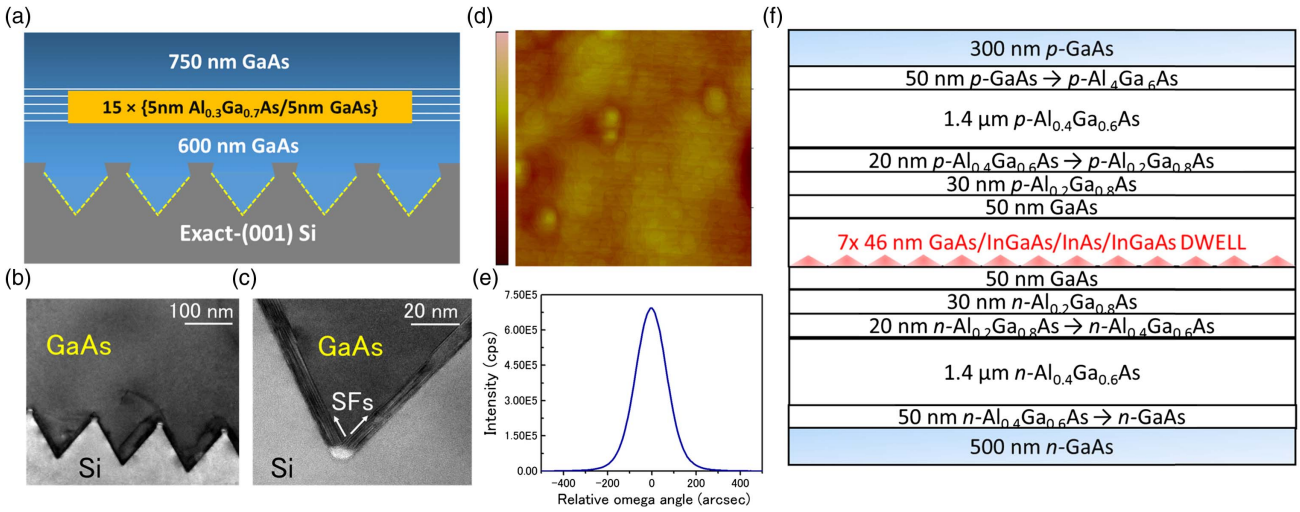

Fig. 1. (a) Schematic of the GaAs-on-Si template. (b) and (c) Cross-sectional TEM images of the V-grooved structure, showing stacking faults trapped by the silicon pockets. (d) AFM image of approximately 1.5 μm coalesced GaAs thin film of the GaAs-on-Si template. The vertical bar is 15 nm. (e) The GaAs (004) rocking curve showing a FWHM value of 162 arcsec. (f) The schematic of the complete epitaxial laser structure.

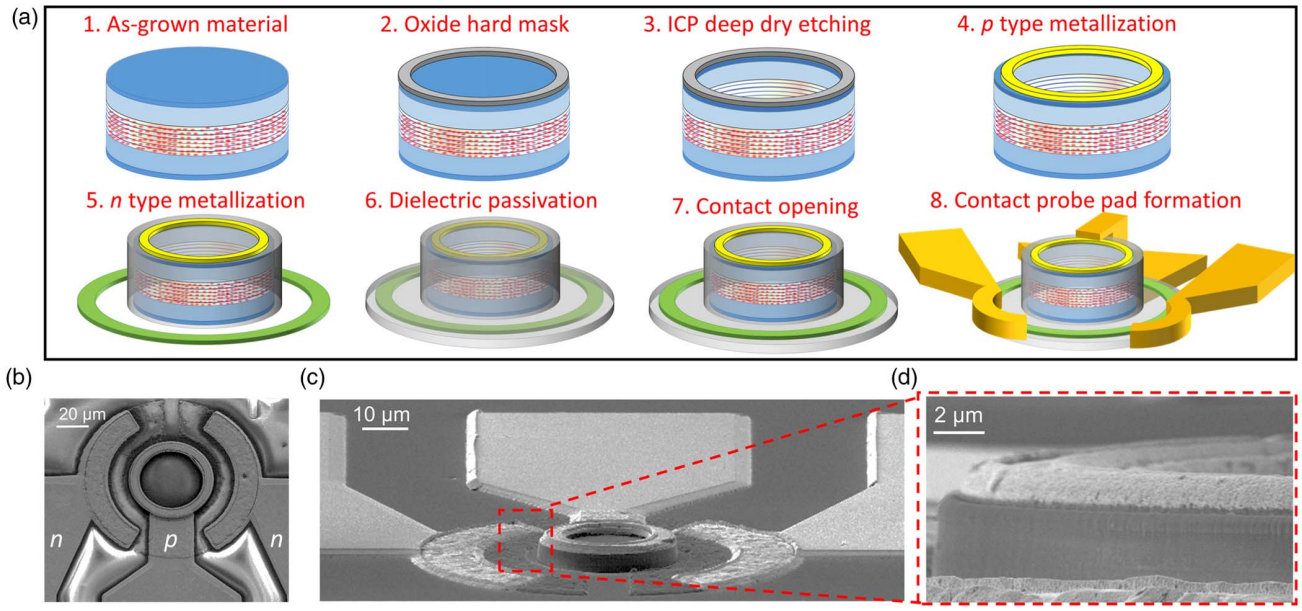

Fig. 2. (a) Processing steps in the device fabrication. Top view (b) and cross-sectional view (c) SEM images of a fabricated device. (d) 90° tilted zoomed-in SEM image of the mesa.

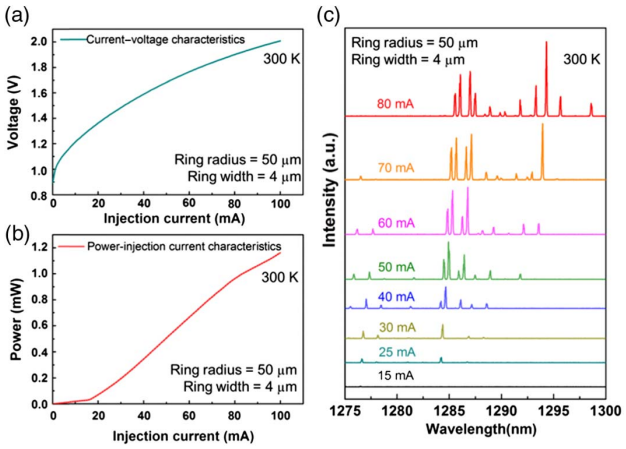

Fig. 3. (a) Current-voltage characteristics, (b) power-injection current characteristics, and (c) emission spectra at progressively higher injection currents for a micro-ring laser with a radius of 50 μm and a ring width of 4 μm under CW operation at room temperature.

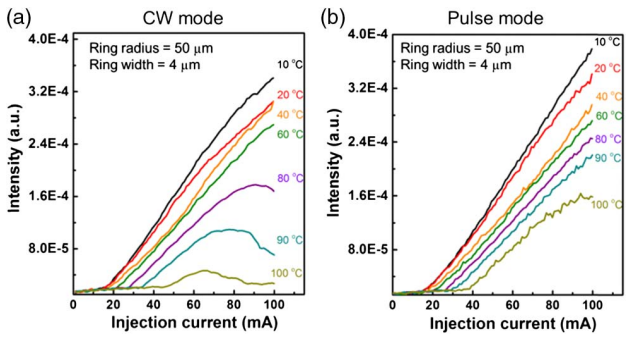

Fig. 4. Measured L–I curve from the micro-ring laser with a radius of 50 μm as a function of temperature under (a) CW operation and (b) pulsed condition.

transition in QDs. The free spectral range (FSR) was calculated for the fundamental transverse mode using the formula of $\Delta\lambda \approx \lambda^2/2\pi R n_g$, wherein n_g is the group refractive index of the cavity, R is the disk radius, and λ represents the emission wavelength. The calculated FSR of 1.56 nm agrees well with the measured FSR of ~1.4 nm.

On-chip lasers for datacom applications are normally required to operate at elevated temperatures up to 80°C, i.e., the processor temperature [18]. We thus tested the same micro-ring laser at various heatsink temperatures and analyzed its L–I characteristic under CW and pulsed operation modes in Figs. 4(a) and 4(b), respectively. For pulsed measurement, we used a 0.5% duty cycle and 5 μs pulse width. The maximum heatsink temperature here is 100°C, limited by the thermoelectric heater.

Figures 5(a) and 5(b) summarize the lasing thresholds and relative slope efficiencies as a function of operating temperature under CW and pulsed operation mode, respectively. Using an exponential function of $P_{\mathrm{th}}\alpha \exp(\frac{T}{T_0})$, the characteristic temperature T_0 was extracted to be 69 K between 10°C and 30°C, 175 K between 30°C and 50°C, and 63 K between 60°C and 100°C under pulsed operation. Under CW operation, the T_0 was similar, i.e., 197 K between 10°C and 50°C and 55 K between 60°C and 100°C. The respective slope efficiency decreased by 45% and

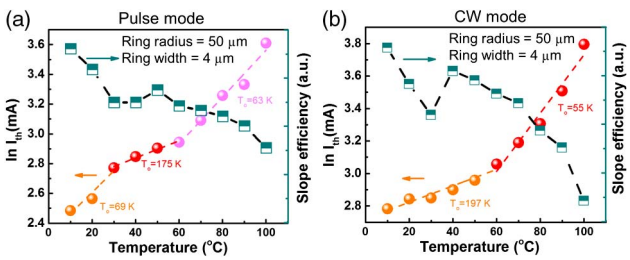

Fig. 5. Temperature dependence of the threshold current and the slope efficiency, from the micro-ring laser with a radius of 50 μm and a ring width of 4 μm under (a) pulse operation and (b) CW condition. The dashed lines represent linear fits to the experimental data.

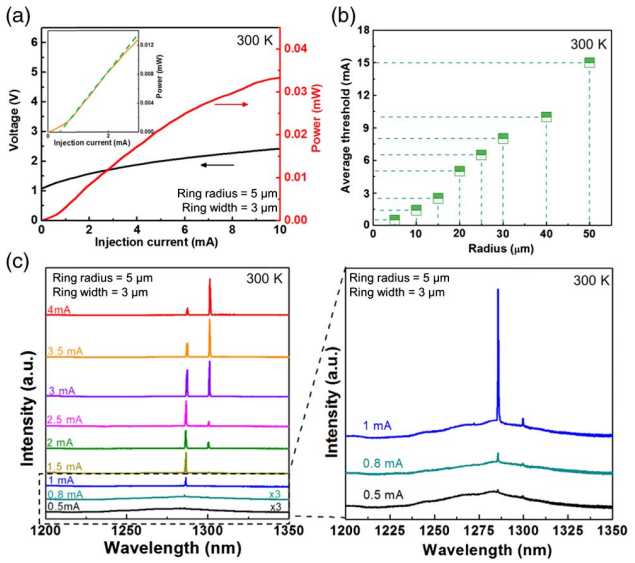

Fig. 6. (a) Measured L–I–V curve of a micro-ring laser with a radius of 5 μm and a ring width of 3 μm. Inset is the zoom-in view of the L–I curve to visualize the onset of the kink. (b) Zoomed-in view of the LI curve in the log–log scale. Inset: infrared image of the laser cavity above threshold. (c) Emission spectra with progressively higher injection currents.

69% for pulsed and CW operation when the heatsink temperature increased from 10°C to 100°C. In general, laser performance will degrade at higher temperatures due to carrier escape from the active region with added thermal energy, leading to efficiency loss and higher thresholds resulting from higher carrier densities in the reservoir outside the quantum dots and increasing opportunity for absorption. The decrease of respective slope efficiency at elevated temperature is thus ascribed to the combined effect of increased non-radiative recombination and reduced gain due to the escape of carriers from QDs. *P*-doping modulation of the QDs active region may reduce the sensitivity of the laser to temperature and optimize the extraction of heat from the active region [17].

For a smaller device with a radius of 5 μm and ring width of 3 μm, an ultra-low threshold ~0.6 mA was measured. The L-I-V curve is presented in Fig. 6(a). The zoomed-in view of the LI curve in the inset of Fig. 6(a) shows the appearance of the lasing kink. Figure 6(b) shows a monotonic decrease of the threshold current with the scaling of the cavity size. This decreasing trend of threshold power density with ring diameter implies no dramatic increase of optical loss or non-radiative recombination that quenches lasing in small cavities [19]. The onset of lasing from the 5 μm ring is evidenced in the emission spectra under progressively higher injection currents, as shown in Fig. 6(c).

4. CONCLUSION

In conclusion, we demonstrate the smallest current injection QD lasers directly grown on industry-standard (001) silicon with low power consumption and high temperature stability. CW lasing around 1.3 μm was achieved with high temperature operation beyond 100°C. Scaling the micro-sized WGM cavity to a radius of 5 μm and a width of 3 μm allows us to realize ultra-low thresholds as small as 0.6 mA. The realization of high-performance micron-sized lasers directly grown on Si represents a major step toward utilization of direct III–V/Si epitaxy as an alternate option to wafer-bonding techniques as on-chip silicon light sources with dense integration and low power consumption. Future work involves integration of in-plane coupling waveguides for efficient extraction/coupling of the lasing light. Continuing work is being conducted to elevate the overall performance of these devices to be comparable to or outperform those achieved by bonding and to integrate these devices with high density in a compact integrated optical communication system.

Funding. Advanced Research Projects Agency—Energy (ARPA-E) (DE-AR0000672); American Institute of Mathematics (AIM); Air Force Research Laboratory (AFRL) (FA8650-15-2-5220); Research Grants Council, University Grants Committee (RGC, UGC) (16212115); Innovation Technology Fund of Hong Kong (ITS/320/14); Hong Kong University of Science and Technology (HKUST).

Acknowledgment. We thank Mike Haney, Minh A. Tran, Chao Xiang, Chen Shang, Lin Chang Mike Davenport, and the UCSB nanofabrication clean room staff for helpful discussions and assistance.

REFERENCES

1. D. Liang and J. E. Bowers, "Recent progress in lasers on silicon," Nat. Photonics **4**, 511–517 (2010).
2. B. Song, C. Stagarescu, S. Ristic, A. Behfar, and J. Klamkin, "3D integrated hybrid silicon laser," Opt. Express **24**, 10435–10444 (2016).
3. S. Chen, W. Li, J. Wu, Q. Jiang, M. Tang, S. Shutts, S. N. Elliott, A. Sobiesierski, A. J. Seeds, I. Ross, P. M. Smowton, and H. Liu, "Electrically pumped continuous-wave III-V quantum dot lasers on silicon," Nat. Photonics **10**, 307–311 (2016).
4. Z. Wang, B. Tian, M. Pantouvaki, W. Guo, P. Absil, J. V. Campenhout, C. Merckling, and D. Van Thourhout, "Room-temperature InP distributed feedback laser array directly grown on silicon," Nat. Photonics **9**, 837–842 (2015).
5. C. Zhang, S. Zhang, J. D. Peters, and J. E. Bowers, "8 × 8 × 40 Gbps fully integrated silicon photonic network on chip," Optica **3**, 785–786 (2016).
6. B. Shi, S. Zhu, Q. Li, Y. Wan, E. L. Hu, and K. May Lau, "Continuous-wave optically pumped 1.55 μm InAs/InAlGaAs quantum dot microdisk lasers epitaxially grown on silicon," ACS Photon. **4**, 204–210 (2017).
7. A. C. Tamboli, E. D. Haberer, R. Sharma, K. H. Lee, S. Nakamura, and E. L. Hu, "Room-temperature continuous-wave lasing in GaN/InGaN microdisks," Nat. Photonics **1**, 61–64 (2007).
8. Y. Wan, Q. Li, A. Y. Liu, A. C. Gossard, J. E. Bowers, E. Hu, and K. M. Lau, "Optically pumped 1.3 μm room-temperature InAs quantum-dot micro-disk lasers directly grown on (001) silicon," Opt. Lett. **41**, 1664–1667 (2016).
9. Y. Wan, Q. Li, A. Y. Liu, A. C. Gossard, J. E. Bowers, E. Hu, and K. M. Lau, "Temperature characteristics of epitaxially grown InAs quantum dot micro-disk lasers on silicon for on-chip light sources," Appl. Phys. Lett. **109**, 011104 (2016).
10. J. Norman, M. J. Kennedy, J. Selvidge, Q. Li, Y. Wan, A. Y. Liu, P. G. Callahan, M. P. Echlin, T. M. Pollock, K. M. Lau, A. C. Gossard, and J. E. Bowers, "Electrically pumped continuous wave quantum dot lasers epitaxially grown on patterned, on-axis (001) Si," Opt. Express **25**, 3927–3934 (2017).
11. D. Liang, M. Fiorentino, T. Okumura, H. Chang, D. T. Spencer, Y. Kuo, A. W. Fang, D. Dai, R. G. Beausoleil, and J. E. Bowers, "Electrically-pumped compact hybrid silicon microring lasers for optical interconnects," Opt. Express **17**, 20355–20364 (2009).
12. N. V. Kryzhanovskaya, M. V. Maximov, A. M. Nadtochiy, S. A. Blokhin, M. A. Bobrov, M. M. Kulagina, S. I. Troshkov, Y. M. Zadiranov, A. A. Lipovskii, E. I. Moiseev, Y. V. Kudashova, V. M. Ustinov, and A. E. Zhukov, "Room temperature continuous wave operation of injection quantum dot microdisk lasers," J. Phys. Conf. Ser. **643**, 012002 (2015).

13. M. Munsch, J. Claudon, N. S. Malik, K. Gilbert, P. Grosse, J. M. Gerard, F. Albert, F. Langer, T. Schlereth, M. M. Pieczarka, S. Hofling, M. Kamp, A. Forchel, and S. Reitzenstein, "Room temperature, continuous wave lasing in microcylinder and microring quantum dot laser diodes," Appl. Phys. Lett. **100**, 031111 (2012).
14. A. Y. Liu, J. Peters, X. Huang, D. Jung, J. Norman, M. L. Lee, A. C. Gossard, and J. E. Bowers, "Electrically pumped continuous-wave 1.3 μm quantum-dot lasers epitaxially grown on on-axis (001) GaP/Si," Opt. Lett. **42**, 338–341 (2017).
15. S. Chen, M. Liao, M. Tang, J. Wu, M. Martin, T. Baron, A. Seeds, and H. Liu, "Electrically pumped continuous-wave 1.3 μm InAs/GaAs quantum dot lasers monolithically grown on on-axis Si (001) substrates," Opt. Express **25**, 4632–4639 (2017).
16. Q. Li, K. W. Ng, and K. M. Lau, "Growing antiphase-domain-free GaAs thin films out of highly ordered planar nanowire arrays on exact (001) silicon," Appl. Phys. Lett. **106**, 072105 (2015).
17. A. Y. Liu, C. Zhang, A. Snyder, D. Lubyshev, J. M. Fastenau, A. W. K. Liu, A. C. Gossard, and J. E. Bowers, "MBE growth of P-doped 1.3 μm InAs quantum dot lasers on silicon," J. Vac. Sci. Technol. B **32**, 02C108 (2014).
18. M. J. R. Heck and J. E. Bowers, "Energy efficient and energy proportional optical interconnects for multi-core processors: driving the need for on-chip sources," IEEE J. Sel. Top. Quantum Electron. **20**, 332–343 (2014).
19. Y. Wan, Q. Li, A. Y. Liu, W. W. Chow, A. C. Gossard, J. E. Bowers, E. Hu, and K. M. Lau, "Sub-wavelength InAs quantum dot micro-disk lasers epitaxially grown on exact Si (001) substrates," Appl. Phys. Lett. **108**, 221101 (2016).